

Research Article

Photosensitization of Colloidal SnO₂ Semiconductor Nanoparticles with Xanthene Dyes

N. Nagarajan, G. Paramaguru, G. Vanitha, and R. Renganathan

School of Chemistry, Bharathidasan University, Tiruchirappalli, Tamil Nadu 620 024, India

Correspondence should be addressed to R. Renganathan; rrengas@gmail.com

Received 2 May 2013; Revised 18 September 2013; Accepted 19 September 2013

Academic Editor: Veysel T. Yilmaz

Copyright © 2013 N. Nagarajan et al. This is an open access article distributed under the Creative Commons Attribution License, which permits unrestricted use, distribution, and reproduction in any medium, provided the original work is properly cited.

The photochemical behavior of xanthene dyes (fluorescein, erythrosine, and eosin) with colloidal SnO₂ nanoparticles was probed by UV-visible, steady state, and time resolved fluorescence measurements. The prepared SnO₂ nanoparticles were characterized by using UV-visible and powder XRD measurements. The xanthene dyes were adsorbed on the surface of colloidal SnO₂ nanoparticles through electrostatic interaction. Apparent association constant (K_{app}) was calculated from the relevant fluorescence data. The larger value of apparent association constant indicates a strong association between xanthene dyes and SnO₂ nanoparticles. The fluorescence quenching is mainly attributed to electron transfer from the excited state xanthenes to the conduction band of colloidal SnO₂. The electron transfer mechanism was explained based on the Rehm-Weller equation as well as the energy level diagram.

1. Introduction

The photosensitization of electron transfer across the semiconductor solution interface plays a vital role in light energy conversion in photoelectrochemical cells, wastewater treatment, nanoelectric devices, silver halide photography, and electrophotography. Effort in this area has concentrated on improving the visible light response of wide-band semiconductors such as SnO₂, ZnO, and TiO₂. Sensitization is achieved by adsorption of dye molecules at the semiconductor surface which, upon excitation, inject an electron into its conduction band [1, 2]. The first successful experiment of this type was described by Putseiko and Terenin [3] who found that the Dember effect of ZnO powder in visible light was sensitized by xanthene and cyanine dyes.

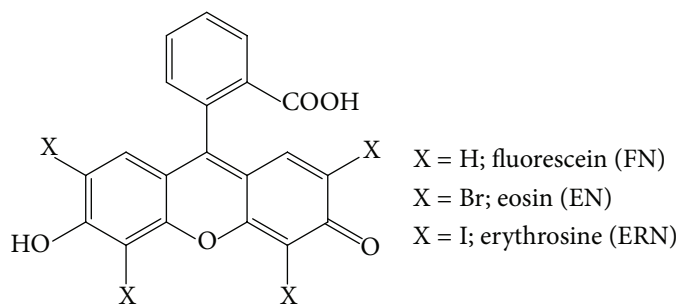
The investigation and development of the dye-semiconductor systems are essential for various fields of applications. Recently Ferrere et al. and Tian et al. used perylene-SnO₂ systems for dye sensitized solar cells [4–6]. The SnO₂ is a stable n-type semiconductor with a wide-band gap ($E_g = 3.6$ eV) being used for various applications, including solid-state gas sensor, photovoltaic devices, dye-based solar cells, transparent conductive films for display and solar cells, catalysis, and anode materials of secondary lithium ion battery [7–9].

Xanthenes belong to the most widely used organic dyes, serving as luminophores [10], molecular probes, bioconjugates, stains, and biologically active substances [11, 12]. These dyes are utilized for photosensitization of redox processes [13, 14] in energy transfer and light sensitization studies [15]. They are also used in light-harvesting dendrimers [16], in biochemistry and medicine as reactants for determination of Zn²⁺, NO [17], and H₂O₂ [18], in sensor devices for H₂S [19], in studying carbon nanotubes [20], for creation of water-soluble fluorescent polymers [21] and new ionic liquids [22–25], and many other fields. Previously we have reported photosensitization of various dyes with semiconductor nanoparticles [26, 27]. The structures of xanthene dyes studied in the present work are shown in Scheme 1.

In the present work, we have studied the interaction between xanthene dyes, namely, fluorescein (FN), eosin (EN), and erythrosine (ERN) with colloidal SnO₂ nanoparticles by using steady state and life time measurements. The electron transfer mechanism is proved by Rehm-Weller equation.

2. Experimental Methods

2.1. Materials. The xanthene dyes were obtained from Aldrich and used without further purification. Dihydrate tin



SCHEME 1

(II) chloride ($\text{SnCl}_2 \cdot 2\text{H}_2\text{O}$) and ethylene glycol (EG) were purchased from Loba, and they were used as such. Double distilled water was used for preparing the solutions throughout. All measurements were performed at ambient temperature.

3. Instrumentation

3.1. Steady-State Measurements. The fluorescence quenching measurements were carried out with JASCO FP-6500 spectrofluorimeter. The slit widths 5 nm and scan rate (500 nm/min) for both excitation and emission were maintained constant for all the measurements. Quartz cells ($4 \times 1 \times 1$ cm) with high vacuum Teflon stopcocks were used for measurements. Absorption spectral measurements were recorded using JASCO V630 UV-visible spectrophotometer.

3.2. Time Resolved Fluorescence Measurements. Fluorescence lifetime measurements were carried out in a picosecond time correlated single photon counting (TCSPC) spectrometer. The excitation source was the tunable Ti-sapphire laser (Tsunami, Spectra Physics, USA). The fluorescence decay was analyzed by using the software provided by IBH (DAS-6).

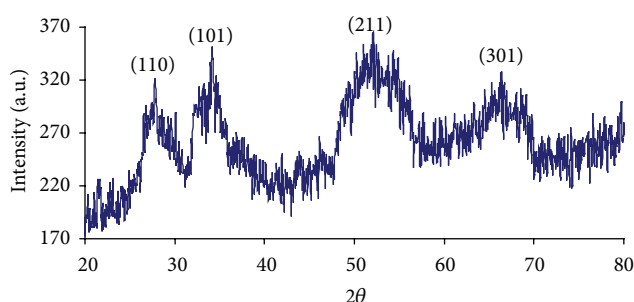
3.3. Powder X-Ray Diffraction Measurements. X-ray diffraction was recorded with a PAN analytical X'Pert Pro MPD X-ray diffractometer using Cu $K\alpha$ radiation ($\lambda = 0.154$ nm) with a Ni filter. The tube current was 30 mA with a tube voltage of 40 kV. The 2θ angular regions between 20 and 80 were explored at a scan rate of 5° min^{-1} .

4. Preparation of Colloidal SnO_2 Nanoparticles

Colloidal SnO_2 nanoparticles were prepared according to the literature method [28]. In a typical procedure, 0.2 g of $\text{SnCl}_2 \cdot 2\text{H}_2\text{O}$ (dissolved in 10 mL of EG) was added to 40 mL of EG that was hosted in a round-bottom flask. After the pH of the solution was kept at 3-4, the solution had been refluxed at 190°C for 2 hours with constant stirring under atmospheric pressure; the clear solution turned into a slight yellow colloid with the reaction time increasing. The resulting SnO_2 colloid was used for the further studies.

5. Results and Discussion

5.1. Determination of Particle Size of Colloidal SnO_2 Nanoparticles. The relationship between band gap shift (ΔE_g) and

FIGURE 1: X-ray diffraction (XRD) spectrum of SnO_2 nanoparticles.

radius (R) of the particles is used to determine the particle size by using Brus equation:

$$\Delta E_g = \frac{\pi^2 \hbar^2}{2\mu R^2} - \frac{1.8e^2}{\epsilon R} + \text{Polarisation term}, \quad (1)$$

where \hbar is the reduced Planck's constant, R is the radius of the particle, μ is the effective reduced masses of the e^- and h^+ in the semiconductor, e is the electron charge, and ϵ is the relative permittivity of the semiconductor.

Reduced effective mass of the exciton ($\mu = 0.275 m_e$) [29] was used for the calculation. A columbic and polarization term in the equation was neglected. The calculated particle size of the prepared colloidal SnO_2 is 1.84 nm.

5.2. XRD Characterization of SnO_2 Nanoparticles. To clarify the crystalline structure, an XRD pattern of the SnO_2 powder is collected and shown in Figure 1. The diffraction peaks at around 27° , 34° , 52° , and 66° are assigned to SnO_2 (110), (101), (211), and (301) (PDF no. 411445), respectively. No diffraction peaks due to metallic Sn or other tin oxides were discerned. The diffraction peaks in the XRD pattern broadened because the particles in the sample are too small. The primary particle size calculated by Scherrer formula is about 1.65 nm.

5.3. Absorption Studies. In an aqueous suspension, the polar surface of metal oxide semiconductor nanoparticles assists adsorption of polar species in solution, and such interactions can lead to absorption spectra changes of these molecules [30, 31]. To find out whether there is any ground state interaction between the sensitizer, that is, xanthene dyes and colloidal SnO_2 nanoparticles, ground state absorption measurements

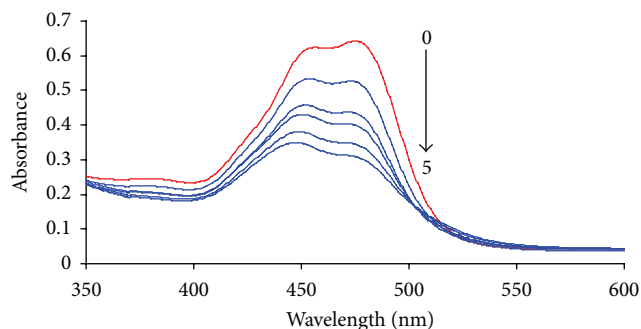


FIGURE 2: Absorption spectrum of FN (1×10^{-5} M; red color) in the presence of colloidal SnO_2 ($0-5 \times 10^{-4}$ M; blue color) in water. The arrow indicates the absorbance decreases on increasing concentration of colloidal SnO_2 .

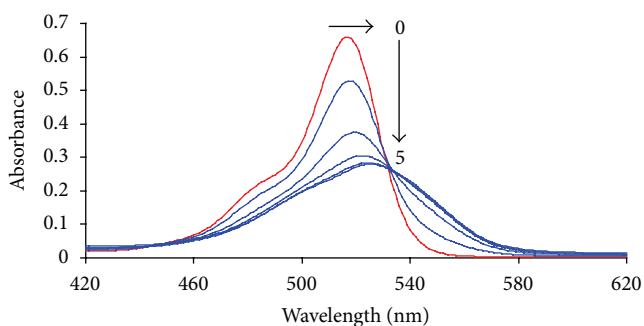


FIGURE 3: Absorption spectrum of EN (1×10^{-5} M; red color) in the presence of colloidal SnO_2 ($0-5 \times 10^{-4}$ M; blue color) in water. The arrow indicates the absorbance decreases with red shift on increasing concentration of colloidal SnO_2 .

of Xanthene in the presence and absence of colloidal SnO_2 nanoparticles have been carried out. Figure 2 shows the absorption spectra of FN (1×10^{-5} M) in water with different concentrations of SnO_2 nanoparticles ($0-5 \times 10^{-4}$ M). Upon increasing the concentration of SnO_2 nanoparticles, the absorption decreases gradually [32]. But EN and ERN show red shift with decrease in absorbance (Figures 3 and 4). The presence of an isosbestic point at 531 nm for EN and 543 nm for ERN in these absorptions shows the existence of dye in the adsorbed and unadsorbed state. Such a red shift of 14 nm and 17 nm in the absorption peak indicates a strong interaction of the dye with SnO_2 surface. Similar spectral changes have been observed for several organic dyes on metal oxide surfaces [33].

5.4. Fluorescence Quenching Studies. The excited state interaction between xanthene dyes and SnO_2 colloid is observed by spectrofluorimetric measurements. Figure 5 shows the emission spectrum of FN in absence and presence of SnO_2 colloid. The fluorescence emission of FN (5×10^{-6} M) was quenched upon successive addition of SnO_2 colloid ($0-5 \times 10^{-5}$ M). Other two dyes also show similar type of spectral behavior (spectra are not shown here). The quenching of

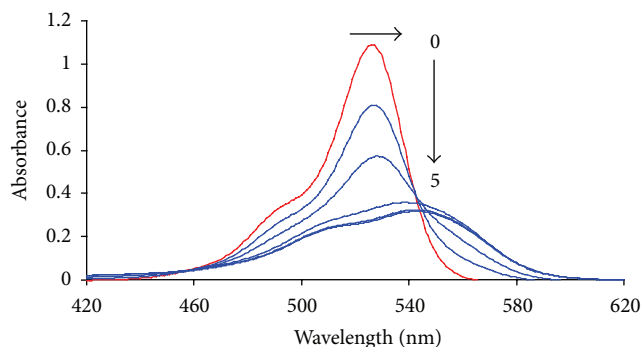


FIGURE 4: Absorption spectrum of ERN (1×10^{-5} M; red color) in the presence of colloidal SnO_2 ($0-5 \times 10^{-4}$ M; blue color) in water. The arrow indicates the absorbance decreases with red shift on increasing concentration of colloidal SnO_2 .

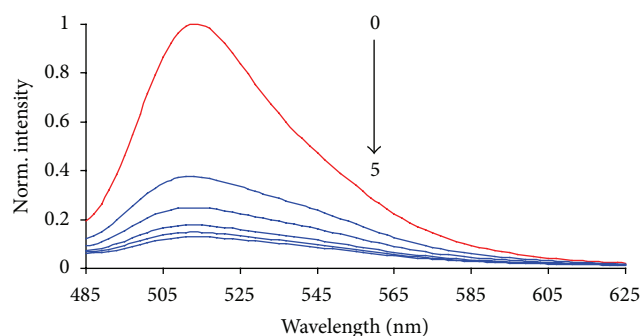


FIGURE 5: Fluorescence quenching of FN (5×10^{-6} M; red color) with colloidal SnO_2 ($0-5 \times 10^{-4}$ M; blue color) in water.

FN fluorescence by SnO_2 colloid can be described by Stern-Volmer:

$$\frac{I_0}{I} = 1 + K_{SV} [Q], \quad (2)$$

where I_0 and I are the fluorescence intensities of xanthene dyes in the absence and presence of SnO_2 colloid, respectively. K_{SV} is Stern-Volmer constant and $[Q]$ is the concentration of respective quencher. The ratios I_0/I were calculated and plotted against quencher concentration according to (2).

The Stern-Volmer plot (Figure 6) for EN and ERN is obtained as upward curvature. These types of upward curvature suggest that it may follow static type of mechanism [34]. But, in the case of FN, it gives linear plot. The linear plot mostly results in dynamic quenching. But its k_q value exceeds ($1 \times 10^{13} \text{ M}^{-1} \text{ s}^{-1}$) the limited values of dynamic quenching ($2 \times 10^{10} \text{ M}^{-1} \text{ s}^{-1}$), so it also may follow the static quenching.

5.5. Fluorescence Lifetime Measurements. In general, time resolved measurement is the most definitive method for differentiating static and dynamic quenching process. Figure 7 presents a representative plot of the logarithm of the relative fluorescence intensity versus time of EN in absence and presence of SnO_2 colloid, from which the lifetimes (τ_f) of the excited singlet states were obtained by iterative deconvolution of the measured instrument response function.

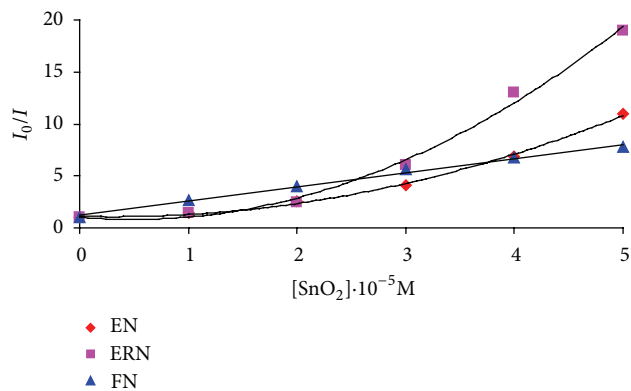


FIGURE 6: Stern-Volmer plot I_0/I versus $[\text{SnO}_2]$ of FN, EN, and ERN dyes.

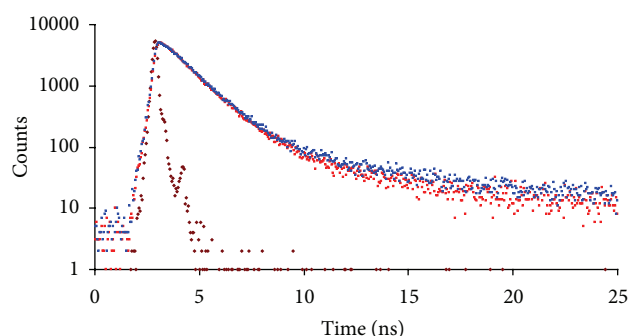


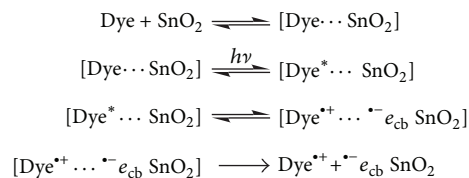
FIGURE 7: Fluorescence decay curve of (i) instrument response curve (Brown color decay), (ii) EN (4×10^{-6} M; red color), and (iii) EN in the presence of colloidal SnO_2 (5×10^{-4} M; blue color).

Fluorescence lifetime observed for EN is unchanged with addition of colloidal SnO_2 . The other two dyes also follow the same trend (spectra are not shown here). This observation shows that quenching follows static mechanism. Static quenching does not decrease the lifetime because only the fluorescent molecules are observed, and the uncomplexed fluorophores have the unquenched lifetime [35]. Static quenching arises due to the formation of complex between fluorophore and the quencher. Hence the association constant (K_{app}) was calculated by the method given below.

The equilibrium between the adsorbed and unadsorbed dye molecules is expressed by using (3); in this equation K_{app} is the apparent association constant which can be calculated from the fluorescence data by using the reported method [31]:

$$\begin{aligned} \text{Dye} + \text{SnO}_2 &\rightleftharpoons \text{Dye} \cdots \text{SnO}_2 \\ K_{\text{app}} &= \frac{[\text{Dye} \cdots \text{SnO}_2]}{[\text{Dye}] \cdot [\text{SnO}_2]} \\ \frac{1}{F_0 - F} &= \frac{1}{F_0 - F'} + \frac{1}{K_{\text{app}}(F_0 - F') [\text{SnO}_2]}, \end{aligned} \quad (3)$$

where K_{app} is the apparent association constant, F_0 is the initial fluorescence intensity of dye molecules, F' is the fluorescence intensity of SnO_2 adsorbed dyes, and F is the observed



SCHEME 2: Schematic diagram describing the conduction and valence band potentials of SnO_2 and the electron-donating energy levels of dyes.

TABLE 1: Excitation (λ_{ex}) and emission (λ_{em}) wavelengths of the xan-thene dyes and apparent association constant (K_{app}) from fluorescence data for dyes with colloidal SnO_2 .

S. number	Dyes	λ_{ex} (nm)	λ_{em} (nm)	$K_{\text{app}} \times 10^3 \text{ M}^{-1}$
1	Fluorescein	478	513	16.6
2	Eosin	517	538	0.8766
3	Erythrosine B	526	550	0.7241

*The uncertainties of the estimated constants are $\pm 6\%$.

fluorescence intensity at its maximum. Figure 8 shows the linear straight line dependence of $1/(F_0 - F)$ on the reciprocal concentration of colloidal SnO_2 . The values are listed in Table 1.

The K_{app} values decrease in the following order:

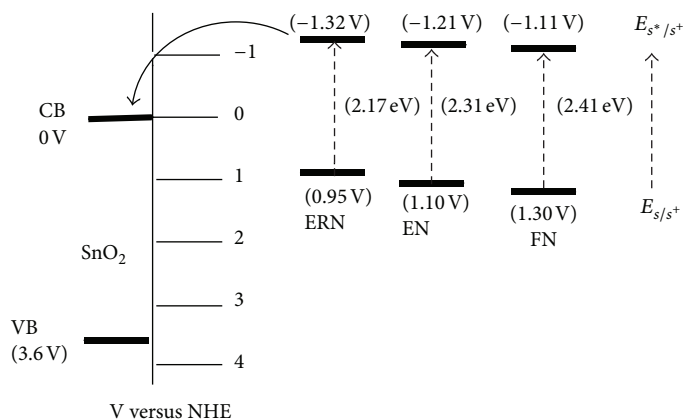
$$\text{FN} > \text{EN} > \text{ERN}.$$

This trend is observed due to the absence of bulkier electronegative group in FN. So the electrostatic interaction between the dye molecule and SnO_2 will be more. So it has higher K_{app} values. But in the case of EN and ERN, it has four bulkier electronegative bromine and iodine atoms. So it has lower K_{app} values.

5.6. Mechanism of Quenching. The fluorescence quenching of dyes by SnO_2 colloid may occur through two possible mechanisms such as energy or electron transfer. There is no overlap between the emission spectra of dyes with the absorption spectrum of SnO_2 colloid (Figure 9), and also the band-gap energy of SnO_2 ($E_g = 3.6 \text{ eV}$) [36] is greater than the excited state energy of dyes (E_s) shown in Table 2. Thus, energy transfer from excited dyes to SnO_2 colloid is not possible. It can therefore be concluded that the fluorescence quenching shown in Figure 5 should not be caused by energy transfer.

The possible way of quenching is through electron transfer from excited state dye molecules to the conduction band of SnO_2 colloid as shown in Scheme 2.

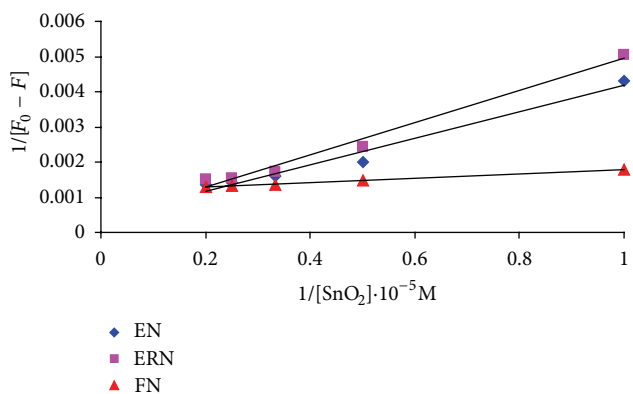
The feasibility of electron transfer from dyes to SnO_2 can be explained on the basis of energy level diagram based on the excited state oxidation potential of dyes obtained from the oxidation potential of dyes and their singlet state energy according to the equation, $E_{s/s^+} = E_{s/s} - E_s$, in Table 2, and the conduction band potential of SnO_2 lies around 0.0 eV as shown in Scheme 3. From the scheme we observed that the electron transfer process is feasible.



SCHEME 3: Proposed electron transfer mechanism.

TABLE 2: Photophysical properties of xanthene dyes.

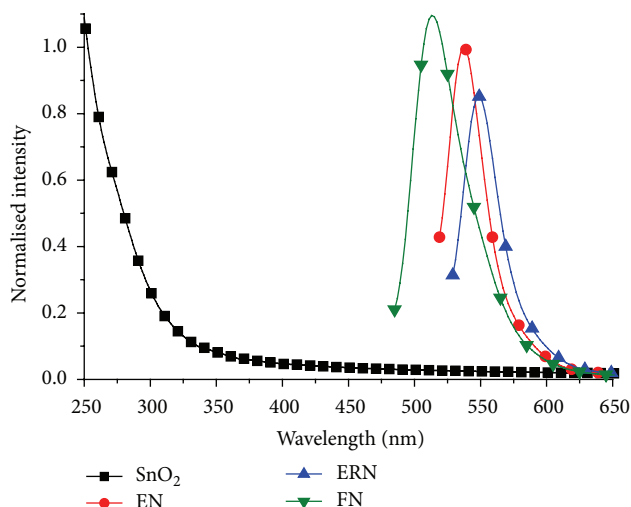
S. no.	Dyes	$E_{(s)}$ (eV) ^a	E_{s/s^+} (V) ^b	E_{s^*/s^+} (V) ^c	ΔG_{et} (eV) ^d
1	Fluorescein	2.41	1.30	-1.11	-1.11
2	Eosin	2.31	1.10	-1.21	-1.21
3	Erythrosine B	2.17	0.95	-1.32	-1.22

^aExcited state energy of the dyes.^bThe oxidation potentials of the ground state dyes in water versus NHE.^cCalculated from the equation, $E_{s^*/s^+} = E_{s/s^+} - E_s$, where E_{s/s^+} is the oxidation potential of the excited state dyes.^dCalculated from the Rehm-Weller equation.FIGURE 8: Linear straight line dependence of $1/F_0 - F$ on the reciprocal concentration of colloidal SnO_2 .

5.7. Calculation of Free Energy Changes (ΔG_{et}) for the Electron Transfer Reactions. To have a better understanding of electron transfer, we have estimated free-energy change (ΔG_{et}) for each dye- SnO_2 systems following Rehm-Weller equation [37]:

$$\Delta G_{et} = E_{1/2}^{(ox)} - E_{1/2}^{(red)} - E_{(s)} + C, \quad (4)$$

where $E_{1/2}^{(ox)}$ is the oxidation potential of the donor, $E_{1/2}^{(red)}$ is the reduction potential of the acceptor, $E_{(s)}$ is the excitation energy of the fluorescent state, and C is the columbic term. Since one of the species is neutral and the solvent used is polar in nature, the columbic term in the above expression is neglected [38]. The ΔG_{et} values thus calculated for

FIGURE 9: Combined absorption spectrum of colloidal SnO_2 (black) and emission spectra of dyes (green: FN, red: EN, and blue: ERN).

the electron transfer processes in the systems studied in water are all negative (Table 2). Hence, the ET processes were thermodynamically feasible [39].

6. Conclusion

The effect of colloidal SnO_2 nanoparticles on the absorption and fluorescence spectra of dyes such as eosin, erythrosine, and fluorescein has been studied. The result in perturbation

of the absorption spectrum shows the surface complex formation through adsorption of dyes on the surface of colloidal SnO_2 . Static nature of quenching has been confirmed by unaltered fluorescence lifetime from time resolved measurements. Based on the energetic calculations the mechanism of electron transfer from excited state dyes to the conduction band of colloidal SnO_2 was suggested.

Conflict of Interests

The authors declare that they have no conflict of interests.

Acknowledgments

N. Nagarajan thanks DST INSPIRE for the fellowship (IF 10495). R. Renganathan and N. Nagarajan thank DST, India, for their financial support in the form of a Research Grant (Ref. no. SR/SI/PC-12/2011, dt. 20/09/2011). Authors also thank UGC/DST-FIST for UV-VIS and Fluorescence facilities in the School of Chemistry, Bharathidasan University. They are thankful to Professor P. Ramamurthy, NCUFP, University of Madras, Chennai for time resolved measurements.

References

- [1] J. Moser and M. Gratzel, "Photosensitized electron injection in colloidal semiconductors," *Journal of the American Chemical Society*, vol. 106, pp. 6557–6564, 1984.
- [2] C. D. Jaeger, F.-R. F. Fan, and A. J. Bard, "Semiconductor electrodes. 26. Spectral sensitization of semiconductors with phthalocyanine," *Journal of the American Chemical Society*, vol. 102, no. 8, pp. 2592–2598, 1980.
- [3] E. K. Putseiko and A. N. Terenin, "Photosensitization of the internal photoeffect in zinc oxide and other semiconductors by adsorbed dyes," *Zhurnal Fizicheskoi Khimii*, vol. 23, p. 676, 1949.
- [4] S. Ferrere, A. Zaban, and B. A. Gregg, "Dye sensitization of nanocrystalline tin oxide by perylene derivatives," *Journal of Physical Chemistry B*, vol. 101, no. 23, pp. 4490–4493, 1997.
- [5] S. Ferrere and B. A. Gregg, "Large increases in photocurrents and solar conversion efficiencies by UV illumination of dye sensitized solar cells," *Journal of Physical Chemistry B*, vol. 105, no. 32, pp. 7602–7605, 2001.
- [6] H. Tian, P.-H. Liu, W. Zhu, E. Gao, D.-J. Wu, and S. Cai, "Synthesis of novel multi-chromophoric soluble perylene derivatives and their photosensitizing properties with wide spectral response for SnO_2 nanoporous electrode," *Journal of Materials Chemistry*, vol. 10, no. 12, pp. 2708–2715, 2000.
- [7] P. Thangadurai, A. C. Bose, S. Ramasamy, R. Kesavamoorthy, and T. R. Ravindran, "High Pressure effects on electrical resistivity and dielectric properties of nanocrystalline SnO_2 ," *Journal of Physics and Chemistry of Solids*, vol. 66, no. 10, pp. 1621–1627, 2005.
- [8] J. A. Toledo-Antonio, R. Gutiérrez-Baez, P. J. Sebastian, and A. Vázquez, "Thermal stability and structural deformation of rutile SnO_2 nanoparticles," *Journal of Solid State Chemistry*, vol. 174, no. 2, pp. 241–248, 2003.
- [9] A. Y. El-Etre and S. M. Reda, "Characterization of nanocrystalline SnO_2 thin film fabricated by electrodeposition method for dye-sensitized solar cell application," *Applied Surface Science*, vol. 256, no. 22, pp. 6601–6606, 2010.
- [10] N. Boens, W. Qin, N. Basarić, A. Orte, E. M. Talavera, and J. M. Alvarez-Pez, "Photophysics of the fluorescent pH indicator BCECF," *Journal of Physical Chemistry A*, vol. 110, no. 30, pp. 9334–9343, 2006.
- [11] R. P. Haugland, *Handbook of Fluorescent Probes and Research Products*, Molecular Probes, Eugene, Ore, USA, 9th edition, 2002.
- [12] A. Zumbuehl, D. Jeannerat, S. E. Martin et al., "An amphotericin B-Fluorescein conjugate as a powerful probe for biochemical studies of the membrane," *Angewandte Chemie International Edition*, vol. 43, no. 39, pp. 5181–5185, 2004.
- [13] D. C. Neckers and O. M. V. Aguilera, "Photochemistry of the xanthene dyes," in *Advances in Photochemistry*, D. H. Volman, G. S. Hammond, and D. C. Neckers, Eds., vol. 18, pp. 313–394, 1993.
- [14] O. Shimizu, J. Watanabe, S. Naito, and Y. Shibata, "Quenching mechanism of rose bengal triplet state involved in photosensitization of oxygen in ethylene glycol," *Journal of Physical Chemistry A*, vol. 110, no. 5, pp. 1735–1739, 2006.
- [15] M. H. V. Werts, J. W. Verhoeven, and J. W. Hofstraat, "Efficient visible light sensitisation of water-soluble near-infrared luminescent lanthanide complexes," *Journal of the Chemical Society*, no. 3, pp. 433–439, 2000.
- [16] V. Balzani, P. Ceroni, S. Gestermann, M. Gorka, C. Kauffmann, and F. Vögtle, "Fluorescent guests hosted in fluorescent dendrimers," *Tetrahedron*, vol. 58, no. 4, pp. 629–637, 2002.
- [17] M. H. Lim, B. A. Wong, W. H. Pitcock Jr., D. Mokshagundam, M.-H. Baik, and S. J. Lippard, "Direct nitric oxide detection in aqueous solution by copper(II) fluorescein complexes," *Journal of the American Chemical Society*, vol. 128, no. 44, pp. 14364–14373, 2006.
- [18] H. Maeda, K. Yamamoto, Y. Nomura et al., "A design of fluorescent probes for superoxide based on a nonredox mechanism," *Journal of the American Chemical Society*, vol. 127, no. 1, pp. 68–69, 2005.
- [19] C. R. Schröder, B. M. Weidgans, and I. Klimant, "pH fluorosensors for use in marine systems," *Analyst*, vol. 130, no. 6, pp. 907–916, 2005.
- [20] N. Nakayama-Ratchford, S. Bangsaruntip, X. Sun, K. Welscher, and H. Dai, "Noncovalent functionalization of carbon nanotubes by fluorescein-polyethylene glycol: supramolecular conjugates with pH-dependent absorbance and fluorescence," *Journal of the American Chemical Society*, vol. 129, no. 9, pp. 2448–2449, 2007.
- [21] H. F. Gao, C. C. Wang, W. L. Yang, and S. K. Fu, "Preparation of a water-soluble fluorescent polymer," *Journal of Macromolecular Science A*, vol. 41, no. 4, pp. 357–371, 2004.
- [22] N. O. McHedlov-Petrosyan, N. A. Vodolazkaya, Y. A. Gurina, W.-C. Sun, and K. R. Gee, "Medium effects on the prototropic equilibria of fluorescein fluoro derivatives in true and organized solution," *Journal of Physical Chemistry B*, vol. 114, no. 13, pp. 4551–4564, 2010.
- [23] J. Pernak, A. Świerczyńska, F. Walkiewicz, E. Krystkowiak, and A. Maciejewski, "Long alkyl chain bis-quaternary ammonium-based ionic liquids as biologically active xanthenes dyes," *Journal of the Brazilian Chemical Society*, vol. 20, no. 5, pp. 839–845, 2009.
- [24] M. Ali, V. Kumar, and S. Pandey, "Unusual fluorescein prototropism within aqueous acidic 1-butyl-3-methylimidazolium tetrafluoroborate solution," *Chemical Communications*, vol. 46, no. 28, pp. 5112–5114, 2010.

- [25] M. Ali, P. Dutta, and S. Pandey, "Effect of ionic liquid on prototropic and solvatochromic behavior of fluorescein," *Journal of Physical Chemistry B*, vol. 114, no. 46, pp. 15042–15051, 2010.
- [26] A. Kathiravan and R. Renganathan, "Effect of anchoring group on the photosensitization of colloidal TiO₂ nanoparticles with porphyrins," *Journal of Colloid and Interface Science*, vol. 331, no. 2, pp. 401–407, 2009.
- [27] M. A. Jhonsi and R. Renganathan, "Investigations on the photoinduced interaction of water soluble thioglycolic acid (TGA) capped CdTe quantum dots with certain porphyrins," *Journal of Colloid and Interface Science*, vol. 344, no. 2, pp. 596–602, 2010.
- [28] L. Jiang, G. Sun, Z. Zhou et al., "Size-controllable synthesis of monodispersed SnO₂ nanoparticles and application in electrocatalysts," *Journal of Physical Chemistry B*, vol. 109, no. 18, pp. 8774–8778, 2005.
- [29] E. J. H. Lee, C. Ribeiro, T. R. Girdali, E. Longo, E. R. Leite, and J. A. Varela, "Photoluminescence in quantum-confined SnO₂ nanocrystals: evidence of free exciton decay," *Applied Physics Letters*, vol. 84, no. 10, pp. 1745–1747, 2004.
- [30] P. V. Kamat, J.-P. Chauvet, and R. W. Fessenden, "Photoelectrochemistry in particulate systems. 4. Photosensitization of a TiO₂ semiconductor with a chlorophyll analogue," *Journal of Physical Chemistry*, vol. 90, no. 7, pp. 1389–1394, 1986.
- [31] P. V. Kamat, "Photoelectrochemistry in particulate systems. 9. Photosensitized reduction in a colloidal titania system using anthracene-9-carboxylate as the sensitizer," *Journal of Physical Chemistry*, vol. 93, no. 2, pp. 859–864, 1989.
- [32] J. Choi, K. Yeo, M. Yoon, S. J. Lee, and K. Kim, "Photoinduced intramolecular charge-transfer state of *p*-dimethylaminobenzoic acid in CdS and TiO₂ colloid solutions," *Journal of Photochemistry and Photobiology A*, vol. 132, no. 1-2, pp. 105–114, 2000.
- [33] P. V. Kamat, S. Das, K. G. Thomas, and M. V. George, "Ultrafast photochemical events associated with the photosensitization properties of a squaraine dye," *Chemical Physics Letters*, vol. 178, no. 1, pp. 75–79, 1991.
- [34] J. Keizer, "Nonlinear fluorescence quenching and the origin of positive curvature in Stern-Volmer plots," *Journal of the American Chemical Society*, vol. 105, no. 6, pp. 1494–1498, 1983.
- [35] J. R. Lakowicz, *Principles of Fluorescence Spectroscopy*, Plenum Press, New York, NY, USA, 1986.
- [36] J.-M. Wu and C.-H. Kuo, "Ultraviolet photodetectors made from SnO₂ nanowires," *Thin Solid Films*, vol. 517, no. 14, pp. 3870–3873, 2009.
- [37] G. J. Kavarnos and N. J. Turro, "Photosensitization by reversible electron transfer: theories, experimental evidence, and examples," *Chemical Reviews*, vol. 86, no. 3, pp. 401–449, 1986.
- [38] S. Parret, F. M. Savary, J. P. Fouassier, and P. Ramamurthy, "Spin-orbit-coupling-induced triplet formation of triphenylpyrylium ion: a flash photolysis study," *Journal of Photochemistry and Photobiology A*, vol. 83, no. 3, pp. 205–209, 1994.
- [39] S. Nath, H. Pal, D. K. Palit, A. V. Sapre, and J. P. Mittal, "Steady-state and time-resolved studies on photoinduced interaction of phenothiazine and 10-methylphenothiazine with chloroalkanes," *Journal of Physical Chemistry A*, vol. 102, no. 29, pp. 5822–5830, 1998.



Hindawi

Submit your manuscripts at
<http://www.hindawi.com>

